

**UCC Library and UCC researchers have made this item openly available.
Please [let us know](#) how this has helped you. Thanks!**

Title	Redox cycling at interdigitated nanowire electrode arrays: enhanced electrochemical sensing
Author(s)	Seymour, Ian P.; Lovera, Pierre; Wahl, Amélie J. C; Rohan, James F.; O'Riordan, Alan
Publication date	2018-07
Original citation	Seymour, I., Lovera, P., Wahl, A., Rohan, J. F. and O'Riordan, A. (2018) 'Redox Cycling at Interdigitated Nanowire Electrode Arrays: Enhanced Electrochemical Sensing', 2018 IEEE 18th International Conference on Nanotechnology (IEEE-NANO), Cork, Ireland, 23-26 July, pp. 1-4. doi: 10.1109/NANO.2018.8626262
Type of publication	Conference item
Link to publisher's version	https://ieeexplore.ieee.org/document/8626262 http://dx.doi.org/10.1109/NANO.2018.8626262 Access to the full text of the published version may require a subscription.
Rights	© 2018 IEEE. Personal use of this material is permitted. Permission from IEEE must be obtained for all other uses, in any current or future media, including reprinting/republishing this material for advertising or promotional purposes, creating new collective works, for resale or redistribution to servers or lists, or reuse of any copyrighted component of this work in other works.
Item downloaded from	http://hdl.handle.net/10468/7665

Downloaded on 2021-05-12T01:01:17Z

Redox Cycling at Interdigitated Nanowire Electrode Arrays: Enhanced Electrochemical Sensing

I. Seymour^{1,2}, P. Lovera², A. Wahl¹, J.F. Rohan¹ and A. O' Riordan^{*2}

¹Electrochemical Materials and Energy Group, Tyndall National Institute, Cork, Ireland

²Nanotechnology Group, Tyndall National Institute, Cork, Ireland alan.*alan.oriordan@tyndall.ie

Abstract—Interdigitated nanowire arrays can be used to perform generator collector type electrochemical measurements. For this set up, one comb of nanowire arrays are used to perform a standard voltammetric technique while the other comb is biased at a constant potential. This technique gives rise to multiple benefits, most notably enhancement of electrochemical signals due to redox cycling, and reduced diffusional overlap in the electrode arrays. Simulations have been used to optimize the electrode designs and to help understand the processes that occur at the electrode surfaces under these conditions. The combination of experimental and simulation data has led to the optimization of a generator collector system with significant collection efficiencies at a variety of conditions.

I. INTRODUCTION

The benefits of using nanoscale electrodes have been well established. Enhanced mass-transport to electrode surface, decreased capacitive currents and increased sensitivities are just a few of the advantages associated with electroanalysis at the nanoscale.^{1, 2} Recent advances in fabrication technology also allow for interesting and useful devices to be developed for nano-electrochemistry applications.^{3, 4} Generator-Collector based approaches using nanoelectrodes are an example of these interesting devices. A generator-collector system is one that consists of two working electrodes in the cell set-up. In general, one of these electrodes undergoes a voltammetric technique while the other is biased at a set potential. The generator electrode typically oxidises or reduces a species to an excited state, while the collector electrode typically reduces or oxidises it back to its ground state.⁵ This approach leads to an effect known as redox cycling (Fig. 1) whereby as the species is bounced back and forth between the generator and collector, significant current amplification is observed leading to increased sensitivities.^{6, 7} Cycling the same species multiple times between the two electrodes means that the same individual molecule can be detected at the generator more than once. This leads to an increase in the current measured for a particular concentration as redox events increase dramatically. This also enables the probing of concentrations much lower than established limits of detection due to the enhancement of measured signal which has been shown for iron in previous work⁸.

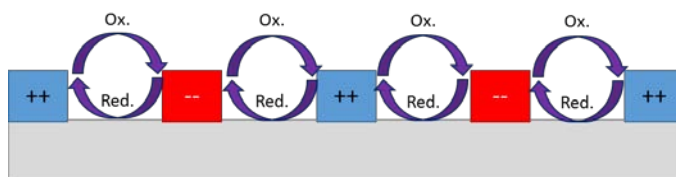


Fig. 1: Schematic representation of redox cycling occurring between generator (blue) and collector (red) electrodes. In this case the generator is positively biased (typically swept up to a positive bias) where an oxidation event can occur. The oxidised species then diffuses across to the negatively biased collector (typically constant potential for duration of analysis) where it reduces and subsequently diffuses back to the generator.

While redox cycling to enhance detection limits is a common application of generator-collector devices, there are many other types of analysis where these devices have uses. Reaction kinetics and diffusional coefficients can be determined by the time taken for a generated species to be collected,^{9, 10} or intermediates and by-products of electrochemical reactions can be analyzed.^{11, 12} Solution conditions can be measured and in some cases adjusted to suit experiment conditions.¹³ Perhaps one of the most attractive emerging features of generator-collector devices is their potential for separating out analytes of interest from interfering species based on their redox reaction kinetics. Consider a situation wherein a solution contains two species A and B both of which oxidise at the same potential on a single electrode. If species A is a reversible redox species and species B is irreversible then the generator electrode will see an increase in signal due to redox cycling of A only when the collector is switched on at the reduction potential of A. Thus the signal increase is due to A alone and this can be calibrated. This can also be applied to species in which the diffusion of one is significantly faster than the other. Simultaneously the current measured at the collector electrode can only be attributed to A as it is the only species that reduces. This method has been used to both separate out interfering species and to also simultaneously measure multiple species of interest.^{6, 14} A limiting factor however of these devices is the collection efficiency. In essence the collector signals depend entirely on what it can detect coming from the generator. In most configurations there are multiple paths that a generated species can take, therefore some (high) losses are expected. Methods to minimise losses and improve efficiency include increasing collector dimensions, decreasing the separation distance

between electrodes and using slower scan rates.¹⁵⁻¹⁷ Collection efficiencies in excess of 90% have been shown at ultramicro- and nano- electrodes however this is typically seen only at extremely slow scan rates.

In this study, a general characterisation was carried out on interdigitated arrays of nano-electrodes visually and electrochemically. The arrays were tested to determine potential enhancement of electrochemical signals by using large arrays with different nano-scale electrode separations. Simulations were performed to aid in the understanding of diffusional processes occurring at the electrode surfaces. Experiments were also performed to compare the collection efficiencies of two arrays of interdigitated electrodes with different generator-collector spacing.

II. MATERIALS AND METHODS

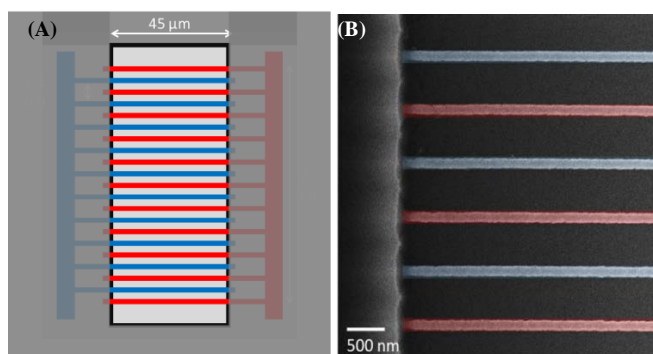


Fig. 2 (a) Schematic representation of the interdigitated electrode arrays. (b) SEM image of the fabricated devices, colour coded blue for Generator and Red for Collector.

The fabrication process used has been shown in previous work for nanowires⁴ and interdigitated arrays⁸. The process itself starts with a Si/SiO₂ wafer onto which an e-beam sensitive resist is spin coated. An e-beam is used to write the pattern for the desired device design. A titanium (10) adhesion layer and a gold layer are deposited by metal evaporation with a typical thickness of between 50 and 100 nm. The pattern is achieved after the excess resist is removed. A photoresist is then spin coated onto the surface and optical lithography is used to write the pattern for the contact pads, interconnection tracks and the counter electrode. Titanium/Gold is again deposited by evaporation and typically a second platinum evaporation is carried out to make the pseudo-reference electrode. The excess resist is again removed. Finally a silicon nitride layer is spin coated and is opened by optical lithography above the arrays, the counter and the reference electrodes to allow access to the electrolyte. Vias are etched in this nitride layer to permit electrical contact with the solution of interest.

Prior to electroanalysis, the electrodes were cleaned by immersion in acetone, iso-propyl alcohol, acetone again and deionised water each for 10 minutes. The devices were housed in a Teflon holder which allowed connection to the contact pads and held the electrolyte. The Teflon holder also had space for an external reference electrode.

Characterisation was performed by scanning the electrodes from 0 to 0.6 V vs SCE reference electrode at 100 mV/s using an Autolab Bipotentiostat in solutions of 1 mM ferrocene carboxylic acid (sigma) in 10 mM phosphate buffered saline (sigma).

III. RESULTS AND DISCUSSIONS

SEM images of an array of interdigitated electrodes in which the separation between generator and collector is shown in Fig. 2(b). This image shows that the electrodes are well resolved without defects, e.g., electrical shorts. The electrodes are well defined and smooth indicating a highly reproducible fabrication process.

Fig. 3 shows a comparison of typical cyclic voltammograms (CV) in 1 mM FcCOOH. The CV shows the redox potential for the Fe²⁺/Fe³⁺ redox couple. The black graph shows a CV performed on a single nanowire and the red graph shows a CV performed on the generator/collector electrodes of a 200 nm gap array. It is clear that the arrays show a much higher current than the single nanowire (9x approx.). However there are significantly more electrodes (137 generators and 138 collectors) in the array so a higher current would be expected, but is not realized due to diffusional overlap occurring at the electrode. Due to the extremely small spacing between electrodes, the diffusion layers at each nanowire expand and overlap causing the array to behave as a single larger electrode. This is confirmed by the quasi diffusion limited behavior seen as a current peak at 0.3 V (diffusion independent would result in steady state currents). Fig. 4 shows a CV where the collector electrode is now biased at 0.01 V. A huge increase in signal is observed. Compared to the array in non-GC mode the current is increased by a factor of 28. This arises from redox cycling. The redox couple is constantly cycling back and forth between the generator and collector leading to a further amplification in current.

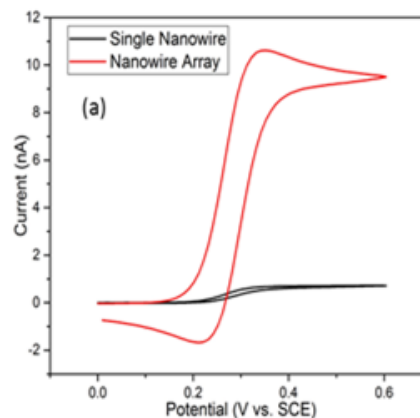


Fig. 3 CVs performed in FcCOOH on a single nanowire (Black) and on one comb of an interdigitated 200 nm gap array.

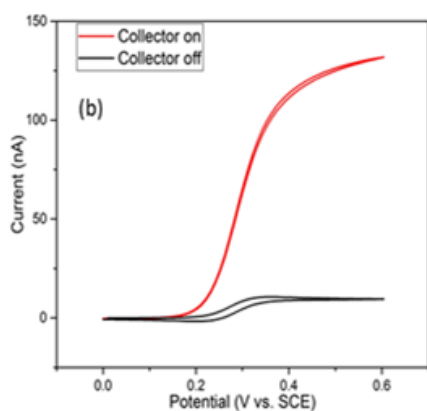


Fig. 4 CV's performed in 1 mM FcCOOH on an array in non-GC mode (black) and on the same array in GC mode (red) with the collector biased at 0.01V

To further prove the source of this current amplification, a simulation study was carried out based on the 200 nm array in the conditions relating to Fig. 4. Comsol Multiphysics was used to simulate the diffusional behavior of FcCOOH in close proximity to the electrode surfaces. Images were recorded at the 25% and 50% mark of the scan corresponding to 3 seconds and 6 seconds after the CV was started (Fig. 5).

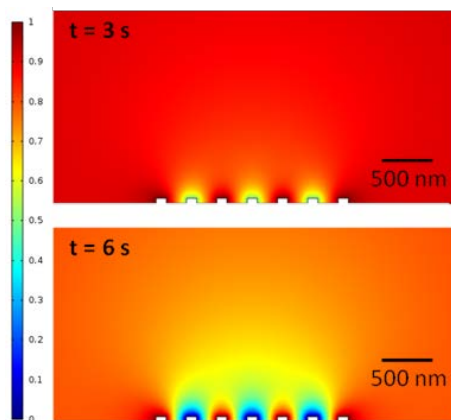


Fig. 5 Simulations recorded at the 3 second and 6 second mark of a CV in FcCOOH. The scale bar illustrates concentration gradients where dark red indicates entirely Fe²⁺ and dark blue indicates entirely Fe³⁺.

As the generator electrode is being swept to more positive potentials, the concentration of Fe²⁺ is shown to decrease. The collector electrode, which in this case is biased at 0.01 V is immediately reducing the produced Fe³⁺ back to its original state. A prominent radial diffusion profile is exhibited by each electrode which explains the increase in current and the steady-state behavior. The simulation also indicates that approximately all of the oxidized species should be collected and cycled back to the generator. This is further confirmed by the experimental data shown in Fig. 6.

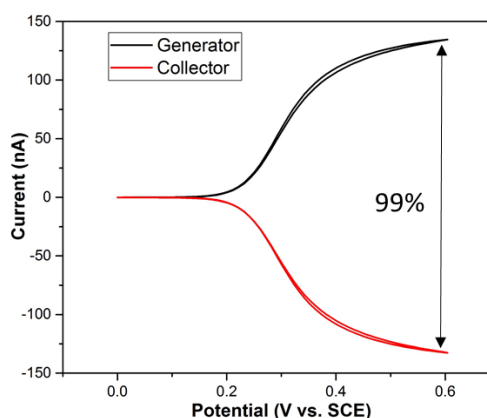


Fig. 6 CV showing both the generator and collector scans in FcCOOH. At 100 mV/s a collection efficiency of 99% was obtained with the 200 nm spacing.

The collection efficiency of generator-collector devices is determined by the peak currents expressed as a ratio of one another. In theory an efficiency of 100% should be obtained, however small amounts of species can diffuse away thus decreasing said efficiency. This leads to a trade-off between analysis time, collection efficiency and electrode spacing. The collection efficiency at a range of scans rates was measured for both a 200 nm and a 500 nm spaced array of interdigitated electrodes. Fig. 7 shows that a 500 nm experiences significant loss in collection efficiency as the scan rate increases. A 200 nm array exposed to the same conditions shows a decrease in efficiency too, however at a much lower rate than the 500 nm array. It is clear that the scan rate could be pushed much higher and potentially still achieve collection efficiencies above 90%.

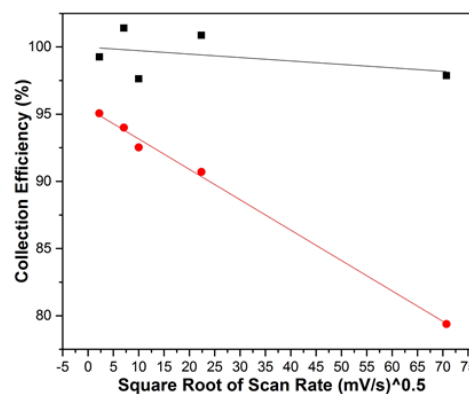


Fig. 7 Comparison collection efficiencies for a 200 nm (black) array and a 500 nm (red) array at increasing scan rates. For the 500 nm array efficiency drops dramatically at higher scan rates.

The collector electrode can also be biased at potentials whereby it can have a direct influence on the conditions observed by the generator electrode. As seen in Fig. 8 biasing the collector at various potentials has a significant impact on the CV at the generator. In the black graph the collector is biased at the starting potential (0.01 V). As the generator electrode oxidises Fe²⁺ to Fe³⁺, the collector subsequently reduces it back to Fe²⁺ and so forth. The red graph shows the effect of biasing the collector at the midpoint potential (0.3 V). In this case the collector electrode is partially oxidising the

surrounding Fe^{2+} initially. When the generator is switched on, it immediately begins reducing this and is swept past the midpoint where it then begins to take over the oxidation process while the collector again reduces. Finally the blue graph shows the effect of biasing the collector at the switching potential (0.6 V). The collector is oxidising the Fe^{2+} fully so the generator electrode is exposed to an environment that is entirely Fe^{3+} . This work highlights the speed at which the influence of one electrode can be detected at the other. In each of the experiments shown in fig. 8, both electrodes were switched on simultaneously with less than 5 seconds before the data began recording. This opens up a wide range of possibilities for analysis wherein a species can be modified at one electrode and subsequently detected at the other. Applications for this type of analysis are in separating out overlapping potential windows of species by exciting one species to a state that can be detected at potentials outside the interfering range.

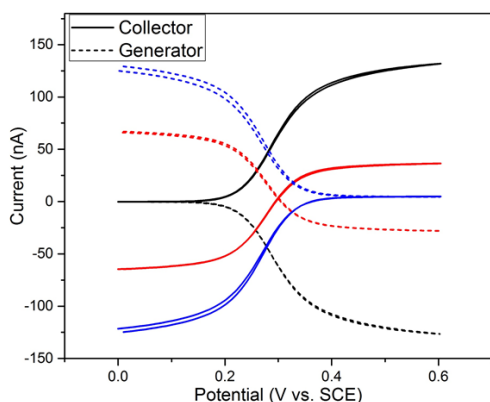


Fig. 8 CVs in FcCOOH wherein the collector is biased at 0 V (black), 0.3 V (red) and 0.6 V (blue).

IV. CONCLUSIONS

In this work we have successfully fabricated interdigitated nanoelectrodes. The generator collector application has been shown to give improvement large increase in signals due to the redox cycling effect. It has also enabled the placing of electrodes significantly closer to each other without leading to diffusional overlap. The collector electrode has also been shown to change local conditions seen at the generator electrode which could potentially be used to separate interferences from analytes based on their redox activity. The 200 nm array spacing has been shown to perform at fast scan rates with no significant loss of collection efficiency. These types of devices could be used for a sensor application wherein fast analysis is essential, such as the detection of contaminants in industrial and pharmaceutical processes.

REFERENCES

1. D. W. M. Arrigan, *Analyst*, 2004, 129, 1157-1165.
2. A. Wahl, S. Barry, K. Dawson, J. MacHale, A. J. Quinn and A. O'Riordan, *Journal of The Electrochemical Society*, 2014, 161, B3055-B3060.
3. Y. Fan, C. Han and B. Zhang, *Analyst*, 2016, 141, 5474-5487.
4. K. Dawson, M. Baudequin, N. Sassiati, A. J. Quinn and A. O'Riordan, *Electrochimica Acta*, 2013, 101, 169-176.
5. E. O. Barnes, G. E. M. Lewis, S. E. C. Dale, F. Marken and R. G. Compton, *Analyst*, 2012, 137, 1068-1081.
6. V. A. T. Dam, W. Olthuis and A. van den Berg, *Analyst*, 2007, 132, 365-370.
7. D. Han, L. P. Zaino, K. Fu and P. W. Bohn, *The Journal of Physical Chemistry C*, 2016, 120, 20634-20641.
8. A. J. C. Wahl, I. P. Seymour, M. Moore, P. Lovera, A. O'Riordan and J. F. Rohan, *Electrochimica Acta*, 2018, 277, 235-243.
9. C. Amatore, C. Sella and L. Thouin, *Journal of Electroanalytical Chemistry*, 2006, 593, 194-202.
10. K. Slowinska, S. W. Feldberg and M. Majda, *Journal of Electroanalytical Chemistry*, 2003, 554-555, 61-69.
11. T. A. Postlethwaite, J. E. Hutchison, R. Murray, B. Fosset and C. Amatore, *Anal. Chem.*, 1996, 68, 2951-2958.
12. B. D. Sherman, M. V. Sheridan, C. J. Dares and T. J. Meyer, *Anal. Chem.*, 2016, 88, 7076-7082.
13. A. K. Dengler, R. M. Wightman and G. S. McCarty, *Anal. Chem.*, 2015, 87, 10556-10564.
14. E. O. Barnes, G. E. M. Lewis, S. E. C. Dale, F. Marken and R. G. Compton, *Journal of Electroanalytical Chemistry*, 2013, 703, 38-44.
15. B. Fosset, C. Amatore, J. Bartelt and R. M. Wightman, *Anal. Chem.*, 1991, 63, 1403-1408.
16. D. Menshykau, F. Javier del Campo, F. X. Muñoz and R. G. Compton, *Sensors and Actuators B: Chemical*, 2009, 138, 362-367.
17. O. Niwa, M. Morita and H. Tabei, *Anal. Chem.*, 1990, 62, 447-452.